Seventh International Conference on CFD in the Minerals and Process Industries
CSIRO, Melbourne, Australia
9-11 December 2009

COMPUTATIONAL FLUID DYNAMICS MODELLING OF POROUS BURNERS

Catharine TIERNEY, Susie WOOD, Andrew T. HARRIS and David F. FLETCHER

School of Chemical and Biomolecular Engineering, University of Sydney, NSW 2006

ABSTRACT

Porous burners offer potential for ultra-lean methane emission mitigation by combustion. In these systems heat recirculation between the porous medium and the fuel stream leads to enhanced combustion behaviour. In this research convective and radiative heat transfer models were added to the commercial computational fluid dynamics (CFD) code ANSYS CFX, to describe the interaction between the porous solid and the fluid. In addition a relatively detailed skeletal chemistry mechanism was incorporated and a stiff chemistry solver was used to provide an accurate assessment of the combustion behaviour. This paper describes the model basis, the skeletal kinetic mechanism and presents example results. The strategy used to obtain converged results from this highly coupled system is also discussed. The methodology used to include heat transfer within a porous matrix in ANSYS CFX provides a useful basis for the examination of porous burner technology and also has wider applicability in the minerals and process industries.

NOMENCLATURE

A_v surface area density [m^{-1}]
c_p specific heat capacity [J kg^{-1} K^{-1}]
d_h hydraulic diameter [m]
D_{km} binary diffusion coefficient [m^2 s^{-1}]
E blackbody intensity [W m^{-2}]
h heat transfer coefficient [W m^{-2} K^{-1}]
h_s surface heat transfer coefficient [W m^{-2} K^{-1}]
h_v volumetric heat transfer coefficient, hA_v [W m^{-3} K^{-1}]
H enthalpy [J kg^{-1}]
I′ radiative intensity [W m^{-2}]
I forward radiation flux [W m^{-2}]
J backward radiation flux [W m^{-2}]
n coordinate, normal direction [m]
N_s number of chemical species
Nu Nusselt number
Re Reynolds number
S source term
t time [s]
T temperature [K]
q nett radiant heat flux [W m^{-2}]
v gas velocity [m s^{-1}]
W molecular weight [kg $mole^{-1}$]
x axial coordinate [m]
Y mass fraction

Γ diffusivity [m^2 s^{-1}]
ε emissivity
ϕ porosity
λ thermal conductivity [W m^{-1} K^{-1}]
μ viscosity [kg m^{-1} s^{-1}]
θ solid angle [rad]
ρ density [kg m^{-3}]
σ Stefan-Boltzmann constant [W m^{-2} K^{-4}]

σ_a absorption coefficient [m^{-1}]
σ_s scattering coefficient [m^{-1}]
τ optical distance [m]
φ radiation flux sum [W m^{-2}]
Ψ diffusive variable [K]
ω molar rate of reaction [mole m^{-3} s^{-1}]

Subscripts:
f fluid phase
i vector component
in inlet
inf infinity
k k-th species
m m-th species
s solid phase
Ts solid temperature component
φ radiation flux sum component
Ψ diffusive variable

INTRODUCTION

An increased focus on fugitive emissions has been created recently by concerns over global warming. Anthropogenic methane (CH_4) emissions, such as those from coal mine ventilation air, are the second highest contributor to the greenhouse effect after carbon dioxide (CO_2) (IPCC, 2007). The high global warming potential of CH_4 is an important factor in its contribution to worldwide greenhouse gas emissions. In fact, CH_4 has 25 times the global warming potential of CO_2, due to its long life and indirect influences (Forster et al., 2007). One method of reducing the impact of these fugitive emissions is to convert the CH_4 to CO_2 via combustion (ACARP, 2007), so as to generate an overall reduction of approximately 89% in global warming potential. Unfortunately, fugitive CH_4 emissions are extremely difficult to combust stably and efficiently, due to the lean CH_4 concentrations and large gas volumes typical of these sources. For example, coal mine ventilation air generally has concentrations of less than 1-vol% CH_4 (US EPA, 2000), which is far below the normal flammability limit, of 5-vol% in air (Glassman, 1996). New combustion techniques for mitigating greenhouse gases from ultra-lean sources are therefore highly desirable.

Porous burners are an exciting development in combustion engineering. These systems no longer rely on traditional

free flames, but contain the combustion reaction within the pores of an inert solid matrix (refer to Figure 1). This innovation produces improved efficiencies, reduced pollutant emissions, an enlarged stable operating power range and, importantly, the ability to operate at concentrations near or below the lower flammability limit (< 5-vol%) (Mossbauer et al., 1999, Trimis and Durst, 1996, Trimis et al., 1997). The properties of the porous materials are crucial to the combustion performance, as they directly influence the degree of heat recirculation occurring in the burner. An improved knowledge of porous burner materials design is necessary to extend the operating range to ultra-lean concentrations.

Figure 1: The heated surface of a porous burner.

Numerical analysis of porous burner technology is required to improve the understanding of the complex interaction of fluid dynamics, chemical reactions and thermal transport within the porous structure. A comprehensive model would augment experimental research, which is limited by restricted measurement techniques and the complexity of the interactions occurring within the burner (Howell et al., 1996, Kiefer et al., 2009). The majority of previous numerical porous burner studies are based upon CHEMKIN (Reaction Design, 2006) and have included examinations of thermal transport (Hackert et al., 1999), material properties (Barra et al., 2003, Kulkarni and Peck, 1996) and the importance of combustion chemistry (Zhou and Pereira, 1998). In other porous burner research, the FASTEST-3D computational fluid dynamics (CFD) software, developed at the University of Erlangen, was used to study hydrocarbon partial oxidation (Al-Hamamre et al., 2007) and the influence of ceramic foam structures upon dispersion (Steven et al., 2007). In other recent work, the ANSYS FLUENT code was used by Liu *et al.* (2009) to model a porous burner, but this research was limited by the use of a global mechanism and diffusive radiant transport. \

In our research, a one-dimensional, computational fluid dynamics model was developed using ANSYS CFX 12.0 (2009), which incorporated the Navier-Stokes equations, solid and fluid energy equations and chemical species transport equations. Separate energy equations were implemented within the porous solid domain, to model heat transport between the phases. A skeletal CH_4 combustion mechanism was incorporated into the model and solved using a coupled chemistry solver. Profiles of temperature and chemical species evolution generated by the model are examined briefly in this paper. The long-term objective of this research is to develop a numerical model for the analysis of materials design in ultra-lean porous burners.

PROBLEM DESCRIPTION

Governing Equations

Conservation equations for mass, momentum, gas phase energy, solid phase energy and species were solved in this problem. Steady, laminar and Newtonian flow was assumed and the porous media was assumed to be homogeneous and inert. The governing equations are given below.

Continuity equation:

$$\nabla.(\phi_f \rho_f \mathbf{v}) = 0 \tag{1}$$

Momentum equation:

$$\nabla.(\phi_f \rho_f \mathbf{v} \otimes \mathbf{v}) = -\phi_f \nabla p + \nabla.(\phi_f \mu \nabla \mathbf{v}) \tag{2}$$

Gas phase energy equation:

$$\nabla.(\phi_f \rho_f H_f \mathbf{v}) = \nabla.(\phi_f \lambda_f \nabla T_f) + h_v (T_s - T_f) - \phi_f \sum_{k=1}^{N_s} \omega_k H_k W_k \tag{3}$$

Solid phase energy equation:

$$0 = \nabla.(\phi_s \lambda_s \nabla T_s) + h_v (T_f - T_s) - \nabla.\mathbf{q} \tag{4}$$

Species conservation equation:

$$\nabla.(\rho_f Y_k \mathbf{v}) = \nabla.(\rho_f D_{km} \nabla Y_k) + \omega_k W_k, \quad k \in [1, N_s] \tag{5}$$

Separate solid and fluid energy equations were considered to accurately model local temperature differences between the solid and gas. The energy equations were coupled through the convective heat transfer term. This term was estimated by Fend *et al.* (2005) for a silicon carbide foam with 81% porosity and 10 pores per inch, using the expressions:

$$Nu = 0.95\, Re^{0.35} \tag{6}$$

$$Nu = h \frac{d_h}{\lambda_f} \tag{7}$$

$$Re = \frac{\rho \phi_f |\mathbf{v}| d_h}{\mu} \tag{8}$$

where Re is the Reynolds number and Nu is the Nusselt number. The hydraulic diameter (d_h) was approximated using the strut diameter of a tetrakaidecahedron-based unit cell, in accordance with Gibson and Ashby (1997). The volumetric heat transfer equation was calculated from:

$$h_v = A_v h \tag{9}$$

Pressure loss due to the presence of the porous matrix was incorporated through the Ergun correlation, as modified by Macdonald (1979):

$$\nabla p = -\left(\frac{180 \phi_s^2 \mu}{\phi_f^3 d_h} \mathbf{v} + \frac{1.8 \phi_s \rho}{\phi_f^3 d_h} |\mathbf{v}| \mathbf{v} \right) \tag{10}$$

The inclusion of radiation absorption by the solid is important for accurate numerical analysis of porous burners (Zhou and Pereira, 1997, Malico and Pereira, 2001). Radiative transfer within the solid matrix was included in the analysis, but gas phase radiation was neglected due to the comparatively low emissivity of the gas. The solid was assumed to be a grey, diffuse and homogeneous medium. The equation of radiative transfer for isotropic scattering is (Viskanta et al., 1966):

$$\cos\theta \frac{dI'(\cos\theta,\tau)}{d\tau} = \left(1 - \frac{\sigma_s}{\sigma_a + \sigma_s}\right)E - I'(\cos\theta,\tau) + \frac{1}{2}\left(\frac{\sigma_s}{\sigma_a + \sigma_s}\right)\int_{-1}^{1} I'(\cos\theta,\tau)d(\cos\theta) \quad (11)$$

where the change in radiation intensity is given on the left hand side of equation (11) and the contributions to this change (emission, absorption and scattering, respectively) are given on the right hand side. The Schuster-Schwarzchild approximation (refer to Modest's (2003) description for example) was used to solve the radiative transfer equation, as it leads to a relatively simple, computationally efficient radiation model. The implementation of this method is described in detail in the following sections.

NUMERICAL MODEL DESCRIPTION

Computational Domain and Material Properties

The laboratory-scale porous burner system shown in Figure 1 provided the physical basis for the model. Accordingly, the one-dimensional model consisted of a 240 mm long domain. This entity was created as a 'porous domain', and was therefore assumed to be a homogenous porous body. The material properties of the porous domain given in Table 1 are representative of a silicon carbide ceramic foam of 81% porosity and 10 pores per inch (Al-Hamamre et al., 2007, Fend et al., 2005, Trimis et al., 2005).

Porosity (ϕ_f)	81%
Hydraulic diameter (d_h)	0.83×10^{-3} m
Area density (A_v)	500 m^{-1}
Thermal conductivity (λ_s)	35 W m^{-1} K^{-1}
Heat capacity (c_{ps})	800 J kg^{-1} K^{-1}
Absorption coefficient (σ_a)	46 m^{-1}
Scattering coefficient (σ_s)	224 m^{-1}
Emissivity	0.9

Table 1 Material properties of the SiC foam modelled

The computational domain was meshed using a uniform 1D stack of 240 hexahedral elements of 1×10^{-3} m height and 1×10^{-4} m^2 cross-sectional area (refer to Figure 2).

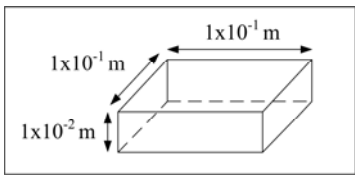

Figure 2: Mesh unit cell

The following boundary conditions were applied: i) gas inlet at the base of the domain, ii) gas outlet at the top surface of the domain, and iii) symmetry boundaries on all other walls.

No additional domain was included to consider the burner outlet surface. It may be necessary to include such a domain in future research to accurately model surface flames that can occur at very low concentrations.

Gas Mixture Properties

A range of ultra-lean mixtures of CH_4 and air were modelled in the burner at 10 atm, using an inlet temperature of 700 K. The four representative cases examined are given in Table 2.

Case	Methane Content (volume %)	Firing Rate (kW/m^2)
1	2.00	150
2	2.00	200
3	2.25	150
4	2.25	200

Table 2 Four representative gas mixture inputs

The firing rate was calculated by multiplying the inlet methane flow rate by its calorific value (39.82×10^6 J m^{-3}) and then dividing this heat release rate by the cross-sectional area of the laboratory scale burner (7.85×10^{-3} m^2).

The mass flow rate and velocity at the inlet for each case is given in Table 3.

Case	Mass Flow Rate (kg s^{-1})	Velocity (m s^{-1})
1	2.20×10^{-5}	5.58×10^{-3}
2	2.94×10^{-5}	7.39×10^{-3}
3	1.96×10^{-5}	5.03×10^{-3}
4	2.61×10^{-5}	6.67×10^{-3}

Table 3 Inlet flow conditions for the four cases

Individual species' thermal conductivity and viscosity values were incorporated into the model using polynomial temperature dependant expressions (Kee et al., 1986). Binary diffusion coefficients were included as temperature and pressure dependant polynomial expressions (Kee et al., 1986). The polynomial inputs were derived from the transport information provided by the GRI3.0 mechanism (Smith et al.).

Numerical Implementation of the Governing Equations

ANSYS CFX 12.0 (2009) does not support heat transfer within the solid and between the phases in a porous domain. Therefore, a number of additional equations were required to incorporate the heat transfer mechanisms within the porous domain.

Modelling Conduction and Convective Transfer within the Porous Domain

Separate solid and fluid energy equations were required in the model, to incorporate solid conduction and convective transfer between the solid and the fluid.

In CFX, the steady-state conservation equation of a diffusive additional variable (Ψ), with units of [K], can be expressed as:

$$\nabla.(\phi_f \rho_f \Gamma \nabla \Psi) + \phi_f S_\Psi = 0 \quad (12)$$

where S_Ψ is the source term and Γ is the diffusivity [m^2 s^{-1}]. Therefore, in comparison with equation (4), conductive transport within a porous solid can be included by setting the diffusive variable to be the solid temperature. The conservation equation becomes:

$$\nabla \cdot (\phi_f \rho_f \Gamma_s \nabla T_s) + \phi_f S_\Psi = 0 \quad (13)$$

where the solid thermal diffusivity of the solid is given by:

$$\Gamma_s = \frac{\lambda_s \phi_s}{\phi_f \rho_f c_{ps}} \quad (14)$$

Equation (14) was incorporated into the model as a kinematic diffusive transport coefficient for the solid temperature (T_s) additional variable.

The source term (S_Ψ) in the conservation equation is related to the heat transfer source (S) by the equation:

$$S_\Psi = \frac{S}{(\phi_f c_{ps})} \quad (15)$$

where the source term for convective transport is:

$$S = hA_v(T_f - T_s) \quad (16)$$

Therefore, the following source terms was added to the CFD model in the fluid energy equation and the solid temperature additional variable equations, respectively:

$$S_f = \frac{hA_v(T_s - T_f)}{\phi_f} \quad (17)$$

$$S_{Ts} = \frac{hA_v(T_f - T_s)}{\phi_f c_{ps}} \quad (18)$$

Source coefficients were set for improved model stability.

Modelling Radiant Transfer within the Porous Domain

Thermal radiation was also included in the domain through the use of a separate additional equation and appropriate source terms. The equation of radiative transfer for isotropic scattering (Equation 11) was solved using the Schuster-Schwarzchild approximation. This method is commonly known as the two flux model when applied in one-dimensional problems. The two flux model is based on the approximation that the radiative intensity (I′) over the solid angle range can be divided into the forward hemisphere and the backward hemisphere, such that:

$$\int_0^1 \cos\theta\, I'(\cos\theta,\tau)\, d\cos\theta \approx \frac{1}{2}\int_0^1 I'(\cos\theta,\tau)\, d(\cos\theta) = I \quad (19)$$

$$\int_{-1}^0 \cos\theta\, I'(\cos\theta,\tau)\, d\cos\theta \approx \frac{1}{2}\int_{-1}^0 I'(\cos\theta,\tau)\, d(\cos\theta) = J \quad (20)$$

where I is the forward radiation flux and J is the backward radiation flux. The approximation creates two separate radiative transfer equations for the forward and backward fluxes, which when substituted into the equation of radiative transfer give:

$$\frac{dI}{dx} = -(\sigma_a + \sigma_s)I + \sigma_a E + \frac{\sigma_s}{2}(I + J) \quad (21)$$

$$\frac{dJ}{dx} = (\sigma_a + \sigma_s)J - \sigma_a E - \frac{\sigma_s}{2}(I + J) \quad (22)$$

Using the radiation flux sum (φ = I+J) these equations can be added to give:

$$\frac{d\varphi}{dx} = (\sigma_a + \sigma_s)(J - I) \quad (23)$$

where the radiative flux sum (φ) is related to the net radiant heat flux (**q**) in the model by:

$$\mathbf{q} = \hat{\mathbf{i}}\varphi \quad (24)$$

Again, a diffusive scalar equation was used to represent the flux sum φ:

$$\frac{d}{dx}\left(\frac{1}{\sigma_a + \sigma_s}\frac{d\varphi}{dx}\right) = \frac{d}{dx}(J - I) \quad (25)$$

which gives upon eliminating J-I:

$$\frac{d}{dx}\left(\frac{1}{\sigma_a + \sigma_s}\frac{d\varphi}{dx}\right) = \sigma_a\varphi - 2\sigma_a E \quad (26)$$

This gives rise to the following source terms, which were implemented in the CFD model in the solid temperature equation and the radiation flux sum equation, respectively:

$$S_{Ts} = \frac{\sigma_a\varphi - 2\sigma_a E}{\phi_f c_{ps}} \quad (27)$$

$$S_\varphi = -\left(\frac{\sigma_a\varphi - 2\sigma_a E}{\phi_f}\right) \quad (28)$$

Source coefficients were again set for improved model stability.

Boundary Conditions

The following boundary conditions were applied in the CFD model, at the inlet:

$$\mathbf{v} = \mathbf{v}_{in};\ T_f = T_{f,in};\ Y_k = Y_{k,in};\ P = P_{in} \quad (29)$$

and, at the outlet:

$$\frac{\partial T_s}{\partial n} = \frac{\partial T_f}{\partial n} = \frac{\partial Y_k}{\partial n} = \frac{\partial P}{\partial n} = 0 \quad (30)$$

At the symmetry boundaries the following conditions were applied:

$$\mathbf{v}_n = \mathbf{0}, \frac{\partial T_s}{\partial n} = \frac{\partial T_f}{\partial n} = \frac{\partial Y_k}{\partial n} = 0 \quad (31)$$

The solid temperature and radiation flux sum boundary conditions were implemented as specified fluxes, to prevent circular referencing of the solid temperature variable when a heat transfer coefficient was used. The solid temperature boundary condition at the inlet was:

$$-\phi_s\lambda_s\frac{\partial T_s}{\partial n} + \varepsilon\sigma(T_{f,in}^4 - T_s^4) + h_s(T_{f,in} - T_s) = 0 \quad (32)$$

and at the outlet:

$$-\phi_s\lambda_s\frac{\partial T_s}{\partial n} + \varepsilon\sigma(T_{inf}^4 - T_s^4) + h_s(T_{inf} - T_s) = 0 \quad (33)$$

The radiation flux sum boundary condition at the inlet is:

$$I - J = \varepsilon\sigma(T_s^4 - T_{f,in}^4) \quad (34)$$

and, at the outlet:

$$I - J = \varepsilon\sigma(T_s^4 - T_{inf}^4) \quad (35)$$

In previous porous burner research (Rumminger, 1996, Shardlow, 1999), the radiation boundary conditions implemented with a two-flux radiation model did not relate logically to the solid temperature boundary conditions. In contrast, the expressions used here are self-consistent.

Chemical Kinetics

The combustion within the porous burner was described by the skeletal mechanism developed by Jazbec *et al.* (2000), which comprises 28 reactions and 12 species. This mechanism was derived from the full mechanism of Bromly *et al.* (1996) at 10 atm, 1000 K and 1-vol% CH_4 in moist air. No other skeletal mechanism is currently available for ultra-lean methane combustion. The Jazbec *et al.* (2000) mechanism was developed specifically for use in CFD analysis and enabled the viability of the porous domain thermal transport model to be demonstrated. A separate low pressure, lean methane combustion mechanism will be developed and implemented in the CFD model in future research.

Solution Method

The commercial CFD code ANSYS CFX 12.0 was used to solve the porous burner model using equations 1-5, 13, 17-18, 24, and 27-28. In order to account for the fast chemical rates, it was necessary to use the stiff chemistry solver, as described by Holm-Christensen *et al.* (2001). In summary, this approach decouples the chemistry and the fluid flow allowing the appropriate solver to be used at each step. Different timescales can also be applied to each solver.

The initial conditions and start-up method were crucial to the successful use of the skeletal mechanism in the model. Initially, a high inlet temperature was used to

cause ignition in the model. The inlet temperature was slowly ramped down to the required value using the iteration number. A converged solution was easily obtained for stable flames. In contrast, mixtures approaching the flammability limits of the burner required additional iterations, based upon an appropriate initial guess.

MODEL VALIDATION

An analytical validation of the heat transfer equations was performed using fixed flux boundary conditions. The analytical temperature distribution coincided with the numerical results exactly. In addition, the validity of the chemical mechanism in the numerical model was confirmed using CHEMKIN (Reaction Design, 2006). This validation was accomplished by imposing a CFD fluid temperature output profile onto a plug flow reactor in CHEMKIN under the same inlet conditions. The CFD profile was obtained without gas transport in accordance with the plug flow reactor conditions. Comparisons of the concentration profiles from CHEMKIN with those from the CFD verified the correct implementation of the chemical mechanism within the CFD model.

RESULTS AND DISCUSSION

The temperature distribution along the burner length, for the gas mixtures examined, is given in Figure 3 and Figure 4. The adiabatic fluid temperature, for the corresponding CH_4 concentration, is also shown.

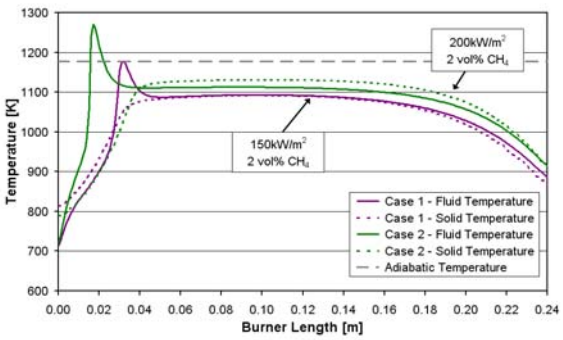

Figure 3: Fluid and solid temperature distributions within the burner model for gas mixtures 1 and 2

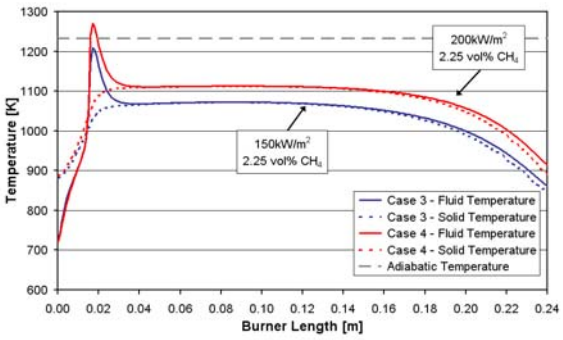

Figure 4: Fluid and solid temperature distributions within the model for gas mixtures 3 and 4

All four gas mixtures have similar temperature profiles. The fluid temperature exhibits a definite peak that coincides with the release of energy from the combustion reaction. It is important to note that the solid phase is hotter than the fluid phase in the entry zone because of internal heat recirculation from the combustion zone. The fluid temperature is observed to peak at values higher than the adiabatic flame temperature when the firing rate is 200 kW/m^2 (cases 2 and 4). This superadiabatic behaviour is typical of efficient lean combustion in porous burners, and occurs when there is a condition of 'excess enthalpy' (Hardesty and Weinberg, 1973). This situation occurs when heat is recirculated from the combustion reaction zone via the solid matrix and acts to preheat the incoming gas mixture through convective transfer. Interestingly, the 150 kW/m^2 gas mixtures (cases 1 and 3) operate subadiabatically, indicating that heat loss at the system boundaries exceeds the energy recirculation.

The combustion behaviour within the porous burner can be investigated by examining the hydrogen radical mole fraction, as this species is associated with carbon dioxide formation in the Jazbec *et al.* (2000) low temperature mechanism. The influence of firing rate and CH_4 concentration upon the hydrogen radical distribution within the burner is shown in Figure 5. The radical distribution profiles are shown in the flame front region (over a shortened length-scale) for clarity.

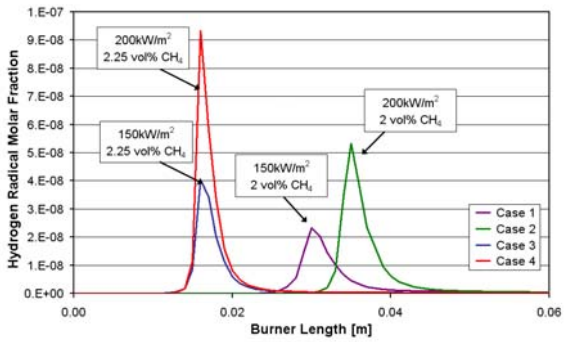

Figure 5: The hydrogen radical molar fraction for the four gas mixture compositions near the flame front

In this research, the combustion zone was observed to relocate downstream (towards the outlet) and be of lower intensity for the 2.00% CH_4 concentration mixtures (cases 1 and 2). The relatively low energy density and higher inlet velocities of the leaner mixtures altered the energy balance within the burner, thereby leading to an altered flame speed and combustion zone location. The peak hydrogen radical concentration was also observed to move further downstream at a firing rate of 200 kW/m^2 (case 2). In this case, the carbon dioxide conversion occurred over a broader reaction zone, as indicated by the corresponding high temperatures observed in the solid temperature profile in Figure 3.

The 200 kW/m^2 mixtures (cases 2 and 4) were observed to have increased intensity combustion behaviour (higher temperatures and hydrogen radical concentrations) compared with the 150 kW/m^2 mixtures (cases 1 and 3). This trend supports the superadiabatic fluid temperatures observed in Figure 3 and Figure 4. In summary, the combustion behaviour observed was directly affected by the energy balance within the system and exhibited behaviour characteristic of porous burners.

CONCLUSIONS AND FUTURE RESEARCH

A rigorous numerical model has been developed that represents the thermal transport occurring within and between the solid and fluid phases of a porous burner. The burner was modelled as a 'porous domain' in ANSYS CFX 12.0 using separate solid and fluid energy equations. Additional equations were included to represent the

thermal transport mechanisms. In particular, conduction within the solid phase, convection between the solid and fluid and solid radiative transfer based on the two-flux approximation were included.

Ultra-lean CH_4/air mixtures were examined using this model with a 10 atm skeletal chemical mechanism. Superadiabatic combustion was observed at a firing rate of 200 kW/m^2 for CH_4 concentrations of 2.00% and 2.25%. The model results indicated that the energy balance of the system determined the combustion performance and flame location. This balance was directly influenced by heat recirculation within the solid matrix and by solid to fluid convective transport.

The successful incorporation of internal heat transfer mechanisms within a porous domain in ANSYS CFX is an important step towards an accurate representation of porous burners. This numerical approach will be used to improve the design of porous burners for ultra-lean combustion and has applicability in a wide range of situations that involve thermal transport in porous media. In the future, the numerical model will be refined through the inclusion of an appropriate atmospheric pressure chemical mechanism and by validation with experimental results. The type and number of materials examined within the burner will also be extended and an exhaust gas domain will be incorporated.

ACKNOWLEDGEMENTS

This work was funded in part by the Australian Coal Association Research Programme. C Tierney was funded by an Australian Government APA scholarship. S Wood was funded by a scholarship from the School of Chemical and Biomolecular Engineering at the University of Sydney. The authors acknowledge the advice of Juan Carlos Morales and Phil Stopford of ANSYS regarding the use of additional variables and the chemistry solver, respectively. The authors are also thankful to Professor Brian Haynes for advice on combustion chemistry.

REFERENCES

ACARP (2007) *Mitigation of Methane in Mine Ventilation Air 2006 Status Report*, Wagner, C. (Eds.), C16049, Australian Coal Association Research Program.

AL-HAMAMRE, Z., VOSS, S. & TRIMIS, D. (2007) Experimental and numerical investigation of the partial oxidation of methane in a porous reactor. In *9th Conference on Energy for a Clean Environment*,

ANSYS (2009) *ANSYS CFX*. v12.0, http://www.ansys.com/products/fluid-dynamics/cfx/.

BARRA, A. J., DIEPVENS, G., ELLZEY, J. L., et al. (2003) Numerical study of the effects of material properties on flame stabilization in a porous burner. *Combustion and Flame*, **134**, 369-379.

BROMLY, J. H., BARNES, F. J., MURIS, S., et al. (1996) Kinetic and thermodynamic sensitivity analysis of the NO-sensitised oxidation of methane. *Combustion Science and Technology*, **115**, 259 - 296.

FEND, T., TRIMIS, D., PITZ-PAAL, R., et al. (2005) Chapter 4.3 - Thermal Properties. In Colombo, P. & Scheffler, M. (Eds.) *Cellular Ceramics*. Chichester Wiley-VCH.

FORSTER, P., RAMASWAMY, V., ARTAXO, P., et al. (2007) Changes in Atmospheric Constituents and in Radiative Forcing. In Solomon, S., Qin, D., et al. (Eds.) *Climate Change 2007: The Physical Science Basis. Contribution of Working Group I to the Fourth Assessment Report of the Intergovernmental Panel on Climate Change*. Cambridge, Cambridge University Press.

GIBSON, L. J. & ASHBY, M. F. (1997) *Cellular Solids - Structure and Properties*, Cambridge, Cambridge University Press.

GLASSMAN, I. (1996) *Combustion*, San Diego, California, Academic Press.

HACKERT, C. L., ELLZEY, J. L. & EZEKOYE, O. A. (1999) Combustion and heat transfer in model two-dimensional porous burners. *Combustion and Flame*, **116**, 177-191.

HARDESTY, D. R. & WEINBERG, F. J. (1973) Burners Producing Large Excess Enthalpies. *Combustion Science and Technology*, **8**, 201 - 214.

HOLM-CHRISTENSEN, O., JONES, I. P., WILKES, N. S., et al. (2001) The solution of coupled flow and chemistry problems. *Progress in Computational Fluid Dynamics*, **1**, 43-49.

HOWELL, J. R., HALL, M. J. & ELLZEY, J. L. (1996) Combustion of hydrocarbon fuels within porous inert media. *Progress in Energy and Combustion Science*, **22**, 121-145.

IPCC (2007) *Climate Change 2007: Synthesis Report*, Core Writing Team, Pachauri, R., et al. (Eds.), Intergovernmental Panel on Climate Change.

JAZBEC, M., FLETCHER, D. F. & HAYNES, B. S. (2000) Simulation of the ignition of lean methane mixtures using CFD modelling and a reduced chemistry mechanism. *Applied Mathematical Modelling*, **24**, 689-696.

KEE, R. J., DIXON-LEWIS, G., WARNATZ, J., et al. (1986) *A Fortran computer code package for the evaluation of gas-phase, multicomponent transport properties*, (Eds.), SAND-86-8246, Sandia National Laboratories.

KIEFER, J., WEIKL, M. C., SEEGER, T., et al. (2009) Non-intrusive gas-phase temperature measurements inside a porous burner using dual-pump CARS. *Proceedings of the Combustion Institute*, **32 II**, 3123-3129.

KULKARNI, M. R. & PECK, R. E. (1996) Analysis of a bilayered porous radiant burner. *Numerical Heat Transfer; Part A: Applications*, **30**, 219-232.

LIU, H., DONG, S., LI, B. W., et al. (2009) Parametric investigations of premixed methane-air combustion in two-section porous media by numerical simulation. *Fuel*, In Press.

MACDONALD, I. F., EL-SAYED, M. S., MOW, K., et al. (1979) Flow through porous media - The Ergun equation revisited. *Industrial and Engineering Chemistry Fundamentals*, **18**, 199-208.

MALICO, I. & PEREIRA, J. C. F. (2001) Numerical study on the influence of radiative properties in porous media combustion. *Journal of Heat Transfer*, **123**, 951-957.

MODEST, M. F. (2003) *Radiative Heat Transfer*, San Diego, USA, Elsevier Science.

MOSSBAUER, S., PICKENACKER, O., PICKENACKER, K., et al. (1999) Application of the porous burner technology in energy- and heat-engineering. In *Fifth International Conference on Technologies and Combustion for a Clean Environment (Clean Air V)*, Lisbon, Portugal.

REACTION DESIGN (2006) *CHEMKIN*. v4.1.1, http://www.reactiondesign.com/products/open/chemkin.html.

RUMMINGER, M. D. (1996) Numerical and experimental investigation of heat transfer and pollutant formation in porous direct-fired radiant burners, PhD thesis, University of California, Berkeley.

SHARDLOW, P. (1999) A one dimensional model for catalysed combustion in a porous burner, ME thesis, University of Sydney.

SMITH, G. P., GOLDEN, D. M., FRENKLACH, M., et al. *GRI-3.0*. http://www.me.berkeley.edu/gri_mech/.

STEVEN, M., MACH, A., VON ISSENDORFF, F., et al. (2007) Numerical simulation of combustion of a low calorific gas mixture in a porous inert medium taking anisotropic dispersion into account. *Third European Combustion Meeting (ECM2007).* Chania, Greece.

TRIMIS, D. & DURST, F. (1996) Combustion in a porous medium - advances and applications. *Combustion Science and Technology*, **121**, 153 - 168.

TRIMIS, D., DURST, F., PICKENACKER, O., et al. (1997) Porous Medium Combustor versus Combustion System with Free Flames. In Wang, S.-P. & Tan, Y.-K. (Eds.) *2nd International Symposium on Heat Transfer Enhancement and Energy Conservation.* Guangzhou, China, South China University of Technology Press.

TRIMIS, D., PICKENACKER, O. & WAWRZINEK, K. (2005) Porous Burners. In Scheffler, M. & Colombo, P. (Eds.) *Cellular Ceramics : Structure, Manufacturing, Properties and Applications* Chichester Wiley-VCH Verlag GmbH.

US EPA (2000) *Technical and Economic Assessment: Mitigation of Methane Emissions from Coal Mine Ventilation Air*, (Eds.), EPA-430-R-001, Agency, U. E. P.

VISKANTA, R., IRVINE, T. F. J. & HARTNETT, J. P. (1966) Radiation Transfer and Interaction of Convection with Radiation Heat Transfer. *Advances in Heat Transfer*. Elsevier.

ZHOU, X. Y. & PEREIRA, J. C. F. (1997) Numerical study of combustion and pollutants formation in inert nonhomogeneous porous media. *Combustion Science and Technology*, **130**, 335-364.

ZHOU, X. Y. & PEREIRA, J. C. F. (1998) Comparison of four combustion models for simulating the premixed combustion in inert porous media. *Fire and Materials*, **22**, 187-197.

